Superior Deep-Ultraviolet Source Pumped by an Electron Beam for NLOS Communication

Yongfeng Kang, Jingyi Zhao, Jiaxin Wu, Lei Zhang, Jian Zhao, Yiqi Zhang, Yuqing Zhao, and Xiaofei Wang

***Abstract*— Deep-ultraviolet (DUV) light ranging from 200 to 280 nm, that is, a solar-blind region, has been widely applied to water purification, sterilization, and integrated biosensors. As the light source for nonline-of-sight (NLOS) communication, DUV light has the natural advantage of a negligible background due to strong ozone absorption. However, the existing DUV sources suffer from either low power or low modulation frequency. Here, we demonstrate a DUV source pumped by an electron beam (EB) at 246 nm with a record-high performance for NLOS communication, that is, a simultaneous continuous-wave output power of 430 mW and a modulation frequency of 5 MHz. Significantly, both the output power and the modulation frequency can be further improved when the horsepower of EBs is fully released. Not only does the proposed DUV source show great capability for NLOS communication and other potential applications, but the EB pumping approach can also be extended to various emission processes.**

***Index Terms*— Deep-ultraviolet (DUV) sources, high luminous power, high-modulation frequency, nonline-of-sight (NLOS) communication.**

I. Introduction

COMMUNICATION technologies have greatly improved information exchange efficiency. In comparison with traditional radio communication using long-wavelength electromagnetic waves, optical wireless communication possesses fruitful frequency resources and an antijamming capability [1]. In particular, deep-ultraviolet (DUV) light ranging from 200 to 280 nm, that is, a solar-blind region, has attracted increasing attention due to its inherent advantages for short-range communication, such as high local security, negligible background, and omnidirectional communication links. Due to the strong scattering effect of small particles or molecules in the atmosphere and even under water, DUV light can be applied to nonline-of-sight (NLOS) communication in a complex terrain environment [1]–[3]. Since the signal decays very quickly, the coverage can be readily controlled by the transmitter power. Therefore, to achieve a high transmission rate, low bit error rate, and relatively long transmission distance, light sources with high luminous power and high-modulation frequency are favorable [4].

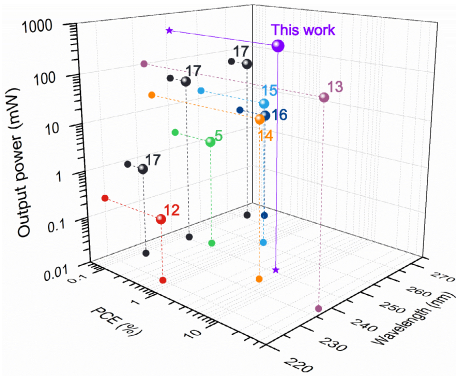

Fig. 1. Recent progress in the development of EB-pumped DUV light sources working in continuous mode. The numbers beside the dots represent their corresponding references.

There are mainly three types of DUV sources, that is, mercury lamps, DUV lasers, and DUV light-emitting devices (LEDs). The former two sources can reach an output power larger than tens of watts. However, their data rate is usually at the level of hundreds of kilobits per second (kbps) or even lower, which mainly results from the difficulty in achieving high-frequency modulation of the sources [5]–[8]. In contrast, $Al_xGa_{1-x}N$-based LEDs have attracted rising consideration because their emission band can be tuned in the range of 210–365 nm by adjusting the doping concentration of the Al component as well as their compact size [9]. Nevertheless, it is still challenging to improve their output power further, especially for wavelengths less than 260 nm, because of several severe inherent issues, such as poor crystalline quality, difficulty in fabricating heavily doped p-type AlGaN with high-Al-content layers, and strong light absorption in p-type GaN injection layers [10], [11]. Although a high output power can be achieved by packaging multiple low-power DUV LEDs in a hybrid connection mode, including both series and shunt connections, a resulted high junction capacitance usually restricts the data rate to kbps within a transmission distance of several hundreds of meters [7], [8].

Manuscript received April 7, 2020; revised May 25, 2020 and June 13, 2020; accepted June 17, 2020. Date of publication July 2, 2020; date of current version July 23, 2020. This work was supported by the National Natural Science Foundation of China under Grant 61671372 and Grant 11604256. The review of this article was arranged by Editor C. Bayram. *(Corresponding authors: Yongfeng Kang; Lei Zhang; Yiqi Zhang.)*

Yongfeng Kang, Jingyi Zhao, Jiaxin Wu, Lei Zhang, Jian Zhao, Yiqi Zhang, and Yuqing Zhao are with the Key Laboratory of Physical Electronics and Devices, Ministry of Education, School of Electronic Science and Engineering, Xi'an Jiaotong University, Xi'an 710049, China (e-mail: yfkang@mail.xjtu.edu.cn; eiezhanglei@mail.xjtu.edu.cn; zhangyiqi@mail.xjtu.edu.cn).

Xiaofei Wang is with the School of Microelectronics, Xi'an Jiaotong University, Xi'an 710049, China.

Color versions of one or more of the figures in this article are available online at http://ieeexplore.ieee.org.

Digital Object Identifier 10.1109/TED.2020.3004122

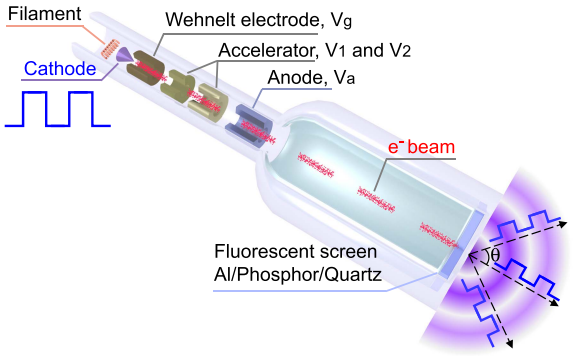

Fig. 2. Schematic of the DUV light source pumped by an EB. After being emitted from a cathode, the EB is engineered by a Wehnelt electrode V_g, two accelerator electrodes V_1 and V_2, and an anode V_a in a vacuum tube. The modulated output emission is controlled by the cathode.

Ongoing endeavors are devoted to improving the performance (output power, modulation frequency, and so on) of DUV light sources. In comparison with the aforementioned approaches, DUV sources pumped by an electron beam (EB) have attracted growing interest in the past decade (see Fig. 1), as they can bypass the challenge of p-type doping [5], [11]–[16]. Lately, by taking advantage of the highly luminous properties of hexagonal boron nitride (hBN), Watanabe *et al.* [12] realized a handheld DUV device with an output power of 0.2 mW at 225 nm excited by a field-emission array. However, the power conversion efficiency (PCE), defined as the ratio of the output power to the input power, is only 0.6%. Subsequently, Oto *et al.* [13] achieved an output power of 100 mW at 240 nm by pumping $Al_xGa_{1-x}N$/AlN quantum wells via an EB with a PCE of 40%. Lately, the output power can be boosted up to 2.2 W at 258 nm under pulsed EB excitation mode with a repetition rate of 50 Hz, where the material quality has been judiciously improved [17]. In fact, due to the high energy carried by electrons, large luminous power is achievable via designing vacuum electronic devices with reasonable structure and appropriate fluorescent materials. Furthermore, by controlling the properties of the EB via applied voltages, the emission power can be readily enhanced in an adjustable way.

Here, we experimentally realize a DUV light source by pumping a layer of yttrium phosphate bismuth ($YPO_4:Bi^{3+}$) film via an EB. By investigating the influence of the applied voltages on the properties of EB both theoretically and experimentally, the performance of the designed DUV source reaches a new level. The DUV source can work in a continuous mode with an output power of 430 mW and a full-width at half-maximum (FWHM) of 16 nm at a wavelength of 246 nm. Moreover, to fulfill the requirement of NLOS communication with a high data rate, a modulation frequency of 5 MHz is demonstrated by varying the voltage applied to the cathode. We believe that our design will not only greatly promote DUV-based applications, but will also ignite the utilization of EBs as a pumping source for other emission processes.

II. Experiment Setup and Principle

Fig. 2 shows a schematic of the EB-pumped DUV light source. The length of the light tube is 145 mm and the radius of the fluorescent screen is 23 mm. $YPO_4:Bi^{3+}$, one type of rare-earth ions doped inorganic luminescence materials, can emit DUV light efficiently with a good thermal stability [18]. In comparison with AlGaN, $YPO_4:Bi^{3+}$ can be readily synthesized chemically, and the emission properties, such as emission peak and fluorescent lifetime, can be well adjusted by controlling the doping level and type of doing elements during synthesis process [19]. In addition, the emission film is obtained by the spin coating method, which facilitates to flexibly control the emission area. The thermal electron emission is launched when a cathode is heated by a filament. Subsequently, an electron optics system, consisting of a Wehnelt electrode, two accelerators, and an anode, is employed to form and adjust the properties of the EB, including the beam current, spot size, and beam energy. In our system, the cathode is connected to the ground if not otherwise specified. Here, by modulating the voltage difference between the cathode and the Wehnelt electrode, the total emitted current can be controlled accordingly, which also offers an achievable approach to modulating the emitted light. Furthermore, two accelerators are adopted to tailor the EB finely, which act as a round electron lens. With an appropriate voltage condition, the anode voltage determines the energy of electrons bombarding the fluorescent screen. The experiment is carried out at room temperature. The vacuum inside the light tube is 10^{-4} Pa. The fluorescent layer, with a thickness of 10 μm, is sandwiched between a 100-nm-thick Al film and a quartz window. After passing the Al film, electrons bombard the fluorescent film. The DUV light then emits outward because the Al film can reflect the backward emission. In addition, the Al film can also help to transfer the residual electrons and prevent the charge-accumulation-induced damage.

In the EB-pumped light emission process, the properties of EBs, including beam current and beam size, play a key role in exciting the DUV light. Therefore, to optimize the DUV emission performance, the properties of the EB are numerically analyzed using a home-developed code based on the equivalent meridional projected trajectory equation and the curvilinear axis evolution theory, which can be applied to calculate the current and charge density distribution of an EB with a rotational symmetry [20]. According to the simulation results, the voltages applied to two accelerators are $V_1 = 20$ V and $V_2 = 200$ V, while the voltage applied to the anode is $V_a = 10$ kV as the initial values in the experiment.

III. DUV Emission

Fig. 3 shows the dependence of the output cathodoluminescence (CL) spectra on the applied voltage of each electrode. A peak at ~246 nm with a narrow FWHM of ~16 nm is observed clearly.

Since the properties of electrons rely on the spatial electric potential distribution, five electrodes are employed to generate the required potentials and then control the track of the EB. A Wehnelt electrode is placed very close to the cathode to achieve efficient control over the electron emission. A reverse electric field will suppress the emission of electrons as well as the light emission. In considering the focusing performance of the electron optics system, the electrons can fully hit the emission screen due to its smaller beam size. Therefore, the increased EB can be totally used to excite the DUV light. As the voltage varies from negative to 0, the emission intensity

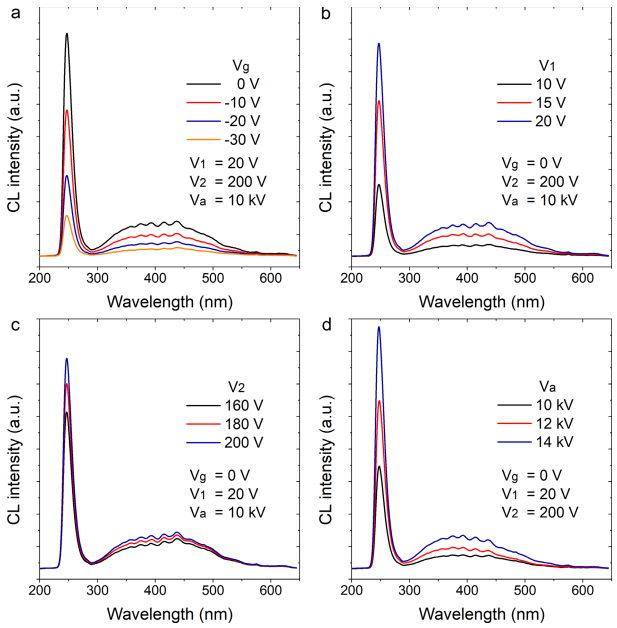

Fig. 3. Dependence of the output CL spectra on each electrode: (a) Wehnelt electrode V_g; (b) accelerator electrode V_1; (c) accelerator electrode V_2; and (d) anode electrode V_a.

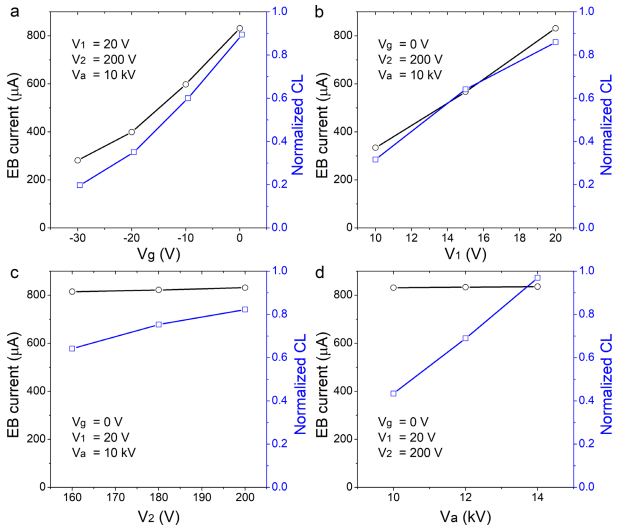

Fig. 4. Dependence of the measured EB current and normalized CL on each electrode: (a) Wehnelt electrode V_g; (b) accelerator electrode V_1; (c) accelerator electrode V_2; and (d) anode electrode V_a.

increases gradually [Fig. 3(a)], since more electrons reach the emission screen [Fig. 4(a)]. The first accelerator electrode V_1 has a similar function to that of the Wehnelt electrode. The emission intensity increases for a large positive voltage V_1 [Figs. 3(b) and 4(b)]. Thereafter, the second accelerator electrode V_2 can finely tune the beam current and beam size. The main function of V_2 is to control the spot size of the EB rather than the beam current [Fig. 4(c)]. The size of the beam spot remains smaller than the screen, which can be estimated using the emission pattern at a broad peak of ~400 nm. As V_2 increases, the size on the fluorescent screen gradually decreases. In our experiment, when $V_2 = 200$ V, the EB almost covers the entire screen, which is beneficial to fully exploit the fluorescent molecules for a larger emission power. On the other hand, for a given input EB current, a small beam spot means

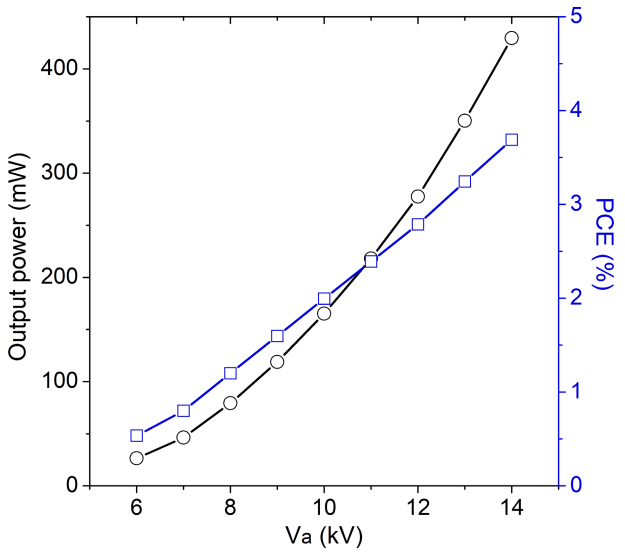

Fig. 5. Dependence of the output power of the light source and the PCE on the anode voltage. Here, $V_g = 0$, $V_1 = 20$ V, and $V_2 = 200$ V.

a high current density, which will increase the brightness of the DUV light. However, due to the low PCE, the fluorescent screen will suffer from a growing risk of damaging caused by accumulated charges and electron–matter interaction-induced heat. Hence, we choose $V_g = 0$ V, $V_1 = 20$ V, and $V_2 = 200$ V as the optimized voltages in our experiment.

After being shaped by the electrodes and gaining adequate kinetic energy via an anode, the electrons still need to penetrate the 100-nm-thick Al film before bombarding the fluorescent molecules. In this process, the energy of electrons will dissipate by 3 keV, which is one cause of low PCE. Subsequently, electrons still carry enough energy to collide with fluorescent molecules multiple times until absorbed or conducted by the Al film. Although the beam current is insensitive to the anode voltage, the CL intensity increases for electrons with higher energy [Figs. 3(d) and 4(d)]. To quantitatively assess the performance of the proposed EB-pumped DUV source, the output power is calculated based on the Lambert distribution [21]. As shown in Fig. 5, both the output power and PCE monotonically increase as the anode voltage increases from 6 to 14 kV, which can be attributed to a deeper penetration of electrons into the fluorescent film and thus a higher electron transition probability. Although the PCE is limited due to the heat dissipation caused by the collisions between electrons and other particles or defects, the output power reaches a record-high value of 430 mW when the voltage $V_a = 14$ kV. In principle, the power can be further upgraded by applying a higher anode voltage. However, low PCE will increase the risk of material damage. Thereby, it is still highly important to improve the PCE and stability for obtaining an excellent DUV source.

IV. Modulation

Since the light emission arises from the excitation by electrons, it is straightforward to realize a light modulation by varying the applied voltage on each electrode. According to the numerical results, when the voltage of the cathode is 10 V, the electron emission will be halted. Consequently, an efficient control over the DUV emission can be achieved by a small

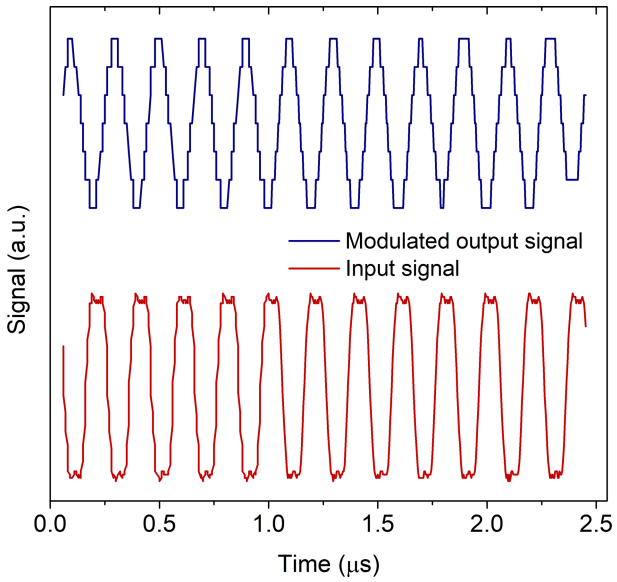

Fig. 6. Modulation of output DUV emission via inputting a square wave signal to the cathode. Here, $V_g = 0$, $V_1 = 20$ V, $V_2 = 200$ V, and $V_a = 14$ kV.

voltage change. To verify the feasibility of the developed DUV source for the NLOS communication system, a pulsed DUV emission is demonstrated. Here, a rectangular voltage with a modulation frequency of 5 MHz is applied to the cathode. The voltage flips between 0 and 10 V in the modulation experiment. As shown in Fig. 6, as the voltage applied to the anode leaps, the output DUV light duplicates the signal shape, where the small deformation can be attributed to the long fluorescent lifetime of $YPO_4:Bi^{3+}$ of ~700 ns. The fluorescent lifetime of the molecule can be further shortened by changing the type of doping element. For example, by replacing Bi with praseodymium (Pr), a lifetime of ~20 ns can be achieved (not shown here), which promises a much faster modulation frequency.

V. Conclusion

To conclude, a high-power and high-modulation-frequency DUV light source is experimentally accomplished by pumping fluorescent molecules with an EB. By judiciously controlling the voltage on each electrode, the emission power can readily achieve a value of 430 mW at 246 nm. Accompanied by a high-modulation frequency of 5 MHz, the proposed DUV source can be a promising candidate for NLOS communications, as well as other areas employing DUV sources. In principle, the performance of the proposed DUV source can be further enhanced by boosting the EB, that is, the beam current and the energy of electrons, and improving the material response. Of more value, not only do our findings pave the way to access NLOS communication and other potential applications, but the EB pumping approach can also be extended to various emission processes.

References

[1] Z. Xu and B. M. Sadler, "Ultraviolet communications: Potential and state-of-the-art," *IEEE Commun. Mag.*, vol. 46, no. 5, pp. 67–73, May 2008, doi: 10.1109/MCOM.2008.4511651.

[2] R. Yuan and J. Ma, "Review of ultraviolet non-line-of-sight communication," *China Commun.*, vol. 13, no. 6, pp. 63–75, Jun. 2016, doi: 10.1109/CC.2016.7513203.

[3] A. Vavoulas, H. G. Sandalidis, N. D. Chatzidiamantis, Z. Xu, and G. K. Karagiannidis, "A survey on ultraviolet C-band (UV-C) communications," *IEEE Commun. Surveys Tuts.*, vol. 21, no. 3, pp. 2111–2133, 3rd Quart., 2019, doi: 10.1109/COMST.2019.2898946.

[4] G. A. Shaw, A. M. Siegel, and J. Model, "Extending the range and performance of non-line-of-sight ultraviolet communication links," *Unattended Ground, Sea, Air Sensor Technol. Appl.*, vol. 6321, May 2006, Art. no. 62310C.

[5] Y. Shimahara *et al.*, "Fabrication of deep-ultraviolet-light-source tube using Si-doped AlGaN," *Appl. Phys. Express*, vol. 4, no. 4, Apr. 2011, Art. no. 042103, doi: 10.1143/APEX.4.042103.

[6] K. W. Kun Wang, C. G. Chen Gong, D. Z. Difan Zou, X. J. Xianqing Jin, A. Z. X., and Z. Xu, "Demonstration of a 400 kbps real-time non-line-of-sight laser-based ultraviolet communication system over 500 m," *Chin. Opt. Lett.*, vol. 15, no. 4, pp. 040602–40605, 2017, doi: 10.3788/COL201715.040602.

[7] G. Wang, K. Wang, C. Gong, D. Zou, Z. Jiang, and Z. Xu, "A 1Mbps real-time NLOS UV scattering communication system with receiver diversity over 1km," *IEEE Photon. J.*, vol. 10, no. 2, 7903013, Apr. 2018, doi: 10.1109/JPHOT.2018.2822690.

[8] Z. Sun, L. Zhang, P. A. Li, Y. Qin, and T. Bai, "1Mbps NLOS solar-blind ultraviolet communication system based on UV-LED array," *Optoelectron. Devices Opt. Signal Process.*, vol. 10617, Jan. 2017, Art. no. 106170O.

[9] M. Kneissl, T.-Y. Seong, J. Han, and H. Amano, "The emergence and prospects of deep-ultraviolet light-emitting diode technologies," *Nature Photon.*, vol. 13, no. 4, pp. 233–244, Apr. 2019, doi: 10.1038/s41566-019-0359-9.

[10] X. Rong *et al.*, "High-output-power ultraviolet light source from quasi-2D GaN quantum structure," *Adv. Mater.*, vol. 28, no. 36, pp. 7978–7983, Sep. 2016, doi: 10.1002/adma.201600990.

[11] D. Li, K. Jiang, X. Sun, and C. Guo, "AlGaN photonics: Recent advances in materials and ultraviolet devices," *Adv. Opt. Photon.*, vol. 10, no. 1, pp. 43–110, 2018, doi: 10.1364/AOP.10.000043.

[12] K. Watanabe, T. Taniguchi, T. Niiyama, K. Miya, and M. Taniguchi, "Far-ultraviolet plane-emission handheld device based on hexagonal boron nitride," *Nature Photon.*, vol. 3, no. 10, pp. 591–594, Oct. 2009, doi: 10.1038/NPHOTON.2009.167.

[13] T. Oto, R. G. Banal, K. Kataoka, M. Funato, and Y. Kawakami, "100 mW deep-ultraviolet emission from aluminium-nitride-based quantum wells pumped by an electron beam," *Nature Photon.*, vol. 4, no. 11, pp. 767–771, Nov. 2010, doi: 10.1038/NPHOTON.2010.220.

[14] T. Matsumoto, S. Iwayama, T. Saito, Y. Kawakami, F. Kubo, and H. Amano, "Handheld deep ultraviolet emission device based on aluminum nitride quantum wells and graphene nanoneedle field emitters," *Opt. Express*, vol. 20, no. 22, pp. 24320–24329, Oct. 2012, doi: 10.1364/OE.20.024320.

[15] F. Fukuyo, S. Ochiai, H. Miyake, K. Hiramatsu, H. Yoshida, and Y. Kobayashi, "Growth and characterization of AlGaN multiple quantum wells for electron-beam target for deep-ultraviolet light sources," *Jpn. J. Appl. Phys.*, vol. 52, no. 1S, Jan. 2013, Art. no. 01AF03, doi: 10.7567/JJAP.52.01AF03.

[16] S. V. Ivanov, V. N. Jmerik, D. V. Nechaev, V. I. Kozlovsky, and M. D. Tiberi, "E-beam pumped mid-UV sources based on MBE-grown AlGaN MQW," *Phys. Status Solidi*, vol. 212, no. 5, pp. 1011–1016, May 2015, doi: 10.1002/pssa.201431756.

[17] Y. Wang *et al.*, "Deep ultraviolet light source from ultrathin GaN/AlN MQW structures with output power over 2 watt," *Adv. Opt. Mater.*, vol. 7, no. 10, May 2019, Art. no. 1801763, doi: 10.1002/adom.201801763.

[18] T. Jästel, P. Huppertz, W. Mayr, and D. U. Wiechert, "Temperature-dependent spectra of YPO4:Me (Me=ce, pr, nd, Bi)," *J. Lumin.*, vol. 106, nos. 3–4, pp. 225–233, Apr. 2004, doi: 10.1016/j.jlumin.2003.10.004.

[19] M. Broxtermann *et al.*, "Cathodoluminescence and Photoluminescence of $YPO_4:Pr^{3+}$, $Y_2SiO_5:Pr^{3+}$, $YBO_3:Pr^{3+}$, and $YPO_4:Bi^{3+}$," *ECS J. Solid State Sci. Technol.*, vol. 6, no. 4, pp. R47–R52, 2017, doi: 10.1149/2.0051704jss.

[20] Y. F. Kang, J. Zhao, J. Y. Zhao, and T. T. Tang, "A novel numerical calculation method for electron guns," *Laser Part. Beams*, vol. 32, no. 3, pp. 487–493, Sep. 2014, doi: 10.1017/S0263034614000421.

[21] W. J. Smith, *Modern Optical Engineering*, 4th ed. Carlsbad, CA, USA: McGraw-Hill, 2007.